

Tests of Chemical Enrichment Scenarios in Ellipticals Using Continuum Colors and Spectroscopy

James Schombert

Department of Physics, University of Oregon, Eugene, OR 97403; js@abyss.uoregon.edu

Karl Rakos

Institute for Astronomy, University of Vienna, A-1180, Wien, Austria; karl.rakos@chello.at

ABSTRACT

We combine spectroscopic metallicity values with integrated narrowband continuum colors to explore the internal metallicity distribution in early-type galaxies. The different techniques for determining metallicity (indices versus colors) allows for an estimate of the contribution from metal-poor stars in a predominantly metal-rich population which, in turn, places constraints on the shape and width of a galaxy's metallicity distribution function (MDF). The color-spectroscopic data is compared to the closed box, infall and inhomogeneous chemical evolution models. The G-dwarf problem, a deficiency in metal-poor stars as compared to closed box models, is evident in the dataset and indicates this deficiency is common to all early-type galaxies. However, even simple infall models predict galaxy colors which are too blue compared to the observations. A simple analytic model is proposed which matches the elliptical data and recent HST observations of M31 (Worthey *et al.* 2005) and NGC 5128 (Harris & Harris 2000) by reducing the number of metal-poor stars in a systematic fashion. While without physical justification, the shape of these models are similar to predictions of inhomogeneous enrichment scenarios.

Subject headings: galaxies: evolution — galaxies: stellar content — galaxies: elliptical

1. INTRODUCTION

The chemical history of galaxies has been a key astrophysics issue since the discovery that our own Galaxy is separated into kinematically distinct regions by metallicity (Baade 1944, Gilmore, Wyse & Kuijken 1989). Due to the process of enrichment by SN and AGB mass-loss, plus a star formation rate that is extended in time, the metallicity distribution function (MDF) in a galaxy evolves with time such that the canonical view of galaxy evolution is that the enrichment process continues to increasingly higher yields until the onset of a galactic wind (powered by SN input) halts star formation (Matteucci 2007). Thus, the MDF of stars becomes a map of past galaxy evolutionary mechanisms.

For nearby galaxies, a direct examination of the color-magnitude diagram (CMD) provides the clearest view of chemical evolution (Dolphin 2002, Skillman *et al.* 2003, Harris & Zaritsky 2004, Grebel 2004). Fortunately, the section of the CMD most sensitive to metallicity effects is the RGB, which is brightest part of a galaxy's CMD and visible to the largest distances. This situation differs from methods to determine a galaxy's age which are dependent on measurements of the fainter turnoff portion of the CMD.

For more distant galaxies, we are forced to deduce the metallicity of the underlying stellar population by comparison of colors or spectral indices interpreted by spectroscopic evolutionary distribution (SED) models. Unfortunately, this type of analysis produces only a luminosity weighted, mean metallicity, although there can be some spatial information (i.e. color gradients). Color information does not resolve the shape of the metallicity distribution, which is a critical piece of information in order to test the type of chemical evolution that a galaxy has undergone.

In the last decade, a series of new techniques to investigate the metallicity of stellar populations in galaxies allows for the possibility of extracting some limited information on the shape of the MDF in ellipticals. It has been noted by several studies that the colors of ellipticals are extremely uniform (Smolcic *et al.* 2006), yet can not be matched with a SED model that is composed of a single metallicity stellar population (Rakos, Schombert & Odell 2008). In addition, their colors, as compared to SED models, indicate a contribution from a bluer (i.e. possibly metal-poor) component (Worthey, Dorman & Jones 1996, Rakos & Schombert 2008), in line with expectations from the MDF of stars in nearby galaxies.

To resolve the effect of a metal-poor population on galaxy colors requires a model of the MDF plus SED spectra of each metallicity bin to sum into an integrated color. In addition, an independent measure of metallicity is required to distinguish the observed value of the colors from the colors present by a population of singular metallicity. Fortunately, just such a measurement of $[\text{Fe}/\text{H}]$ exists from spectroscopic studies, the $\langle \text{Fe} \rangle$ index. This index has the advantage of skipping the need for SED models (although an MDF will produce a luminosity averaged value of $\langle \text{Fe} \rangle$) and directly measures the abundance of Fe. Since Fe is the primary contributor to line blanketing on the RGB, it is also the primary link to color changes in galaxies from metallicity effects.

The goal of this project is to take advantage of the different manner in which metallicity is determined in galaxies (i.e. colors versus spectroscopy) to deduce the basic shape of the MDF in early-type galaxies. To achieve this goal, we will require a series of predicted MDF's, given by various chemical evolutionary scenarios, combined with SED models to calculate the expected galaxy colors. Thus, we will first examine the quality of the current generation of SED models with respect to globular clusters colors and metallicity for a set of special narrowband and near-IR filters (a modified Strömgren system, Rakos & Schombert 1995). Second, we will present a subset of galaxies from spectroscopic studies where we have matching narrowband colors, and explore the behavior of color versus $\langle \text{Fe} \rangle$ for this sample. Lastly, we will compare the resulting $[\text{M}/\text{H}]$ versus color plane with respect to the predictions of various chemical evolution scenarios (such as closed box, infall, inhomogeneous) in order to determine which scenario most closely matches the data.

2. Analysis of SED Models

In order to interpret the global colors or line indices in galaxies, one needs 1) a star formation history model which includes not only a star formation rate but a chemical enrichment model so that a present-day galaxy is characterised by the sum of light from stars with a range of age and metallicity plus 2) accurate SED's for each stellar population of a particular age and metallicity. Clearly, we wish to deduce the star formation history of a galaxy by first determining the present-day mixture of internal stellar populations parameterized by their mean age and mean metallicities. These stellar populations

have unique luminosities by mass which can be summed to determine the total color (or luminosity weighted line indice) for the galaxy.

The first step in unraveling the underlying populations in galaxies is to test the predictions of the various SED models in the literature against systems where we have detailed knowledge of the age and metallicity of the stars (i.e. stellar clusters). The SED models take on the simplest assumptions, a single burst resulting in a population with a single value for their age and metallicity ($[M/H]$), a so-called single stellar populations (SSP). Their direct comparison to galaxy colors is problematic as galaxies cannot be composed of a single burst population simply due to the physics of initial galaxy formation as demonstrated by the discovery of color/metallicity gradients across all Hubble types (see §2.2).

There have been numerous SED models published in the literature since the earliest attempts to model galaxies (Faber 1972, O’Connell 1976, Pickles 1985). Our own narrowband photometry work (Rakos, Schombert & Odell 2008) has focused on the Bruzual & Charlot (2003, hereafter BC03) models and the models from the Gottingen group (Schulz *et al.* 2002). The choice of these two groups was for convenience as we used the original Bruzual & Charlot models for our study of distant clusters (Rakos & Schombert 1995) and we later switched to the Gottingen models since they published Strömgren colors ($uvby$) that were easy to transform into our modified Strömgren system (uz,vz,bz,yz). The adoption of the latest stellar tracks from the Padova group (Girardi *et al.* 2000) by both BC03 and Schulz has rendered their models to be nearly identical with only minor differences in resulting colors and line indices. Thus, for the remainder of this paper we will use the model tracks from BC03 for our analysis and only note the differences between the BC03 and Schulz models where relevant.

For this work, we have selected a fairly standard range of models with an age of 12 Gyrs and $[Fe/H]$ from -2.3 to $+0.4$, all using the Chabrier (2003) IMF (mass cutoff at 0.1 and 100 M_{\odot}) and Padova (2000) isochrones. Each SSP is interpolated at the 0.1 dex level in metallicity and convolved to our narrow band filters to produce a full grid of colors. These SSP’s are then convolved into our various metallicity distribution models as will be discussed in a later section.

2.1. Comparison of SSP Models to Globular Clusters

There do exist stellar systems which closely resemble the narrow conditions of an SSP, the globular clusters of our own Galaxy (hereafter GC’s). Their limited range of internal metallicity and age, as determined from detail studies of their color-magnitude diagrams (CMD), indicates a constant metallicity to within $\Delta[Fe/H] < 0.2$ and spread in internal age of less than 1 Gyr (Bruzual 2002).

A first test to the accuracy of an SED model is to match to the isochrones of globular clusters, for which the modern formulations in the literature are all adequate (see the analysis in Schiavon 2007). Second, is to match the integrated colors of SSP’s to colors of globular clusters. With respect to the BC03 models, there is an excellent discussion of the model fits, as compared to broadband colors, in Bruzual (2002).

As our work deals with integrated narrowband colors, we have collected a sample of 32 GC’s with high quality narrowband colors (uz,vz,bz,yz , Rakos & Schombert 2005) and combined this sample with a subset of GC’s with near-IR colors from Cohen *et al.* (2007). The resulting six color-color diagrams are shown in Figure 1 along with the SSP models of BC03 for an age of 12 Gyrs. The change in color

is due solely to changes in metallicity ($[\text{Fe}/\text{H}]$) as the range of age for GC's is less than 2 Gyrs (Salaris & Weiss 1998) and there is a negligible change in the SSP models for this age range. Note that the uz, vz, bz, yz differs from the normal Strömgren ($uvby$) system in the sense that the filters are slightly narrower (by 20\AA) and the uz filter is shifted 30\AA to the red in its central wavelength as compared to the original system. The uz, vz, bz, yz system covers three regions in the near-UV and blue portion of the spectrum. The first region is longward of 4600\AA , where in the influence of absorption lines is small. This is characteristic of the bz and yz filters ($\lambda_{eff} = 4675\text{\AA}$ and 5500\AA). The second region is a band shortward of 4600\AA , but above the Balmer discontinuity. This region is strongly influenced by metal absorption lines (i.e. Fe, CN) particularly for spectral classes F to M, which dominate the contribution of light in old stellar populations. This region is exploited by the vz filter ($\lambda_{eff} = 4100\text{\AA}$). The third region is a band shortward of the Balmer discontinuity or below the effective limit of crowding of the Balmer absorption lines. This region is explored by the uz filter ($\lambda_{eff} = 3500\text{\AA}$).

The scatter in optical and near-IR colors is relatively large considering the photometric accuracy of the observations. However, this is not a statement concerning the quality of the models but rather an observation effect due to the stochastic aspect of stellar light from GC's. While a GC may be composed of over 10^5 stars, the stars at the tip of the asymptotic giant branch (AGB) and horizontal branch (HB) dominate the integrated light and, therefore, small variations in the number of these stars can dramatically alter the measured colors (see an excellent discussion of this effect in Bruzual & Charlot 2003). Given this stochastic scatter, the models display a good match to the GC colors. The only serious discrepancy is found in the $J - K$ color, for reasons that are not immediately apparent. The clearest correlation in color is found between our two optical colors ($vz - yz$, $bz - yz$) and the near-IR $V - K$ color. These are the three colors most sensitive to metallicity changes and it is not surprising to find them strongly correlated.

The correlations between color and metallicity are shown in Figure 2, plots of color versus $[\text{Fe}/\text{H}]$. For consistency, we have adopted a calibration from the total metallicity ($[\text{M}/\text{H}]$) from $[\text{Fe}/\text{H}]$ based on the Padova 2000 tracks (Girardi *et al.* 2000, discussed in Bruzual & Charlot (2003)). From these plots, it is clear that colors in the near-UV region of the spectrum are degenerate with respect to metallicity. Near-IR colors are well fit by the models, but have shallow slopes at low metallicities making their use problematic. The steepest slopes are seen in $vz - yz$ and $bz - yz$, with the tightest correlation found for $vz - yz$. This confirms what we have learned in our earlier studies on the uniformity in color for ellipticals and the correlations with galaxy mass (i.e. the color-magnitude relation, Odell, Schombert & Rakos 2002). As our previous work on the age and metallicity of ellipticals has demonstrated (Rakos, Schombert & Odell 2008), the range of age in ellipticals is very limited and the majority have mean ages greater than 10 Gyrs. For these ages, $vz - yz$ is strictly a measure of metallicity and, thus, becomes our primary tool for determining metallicity in SSP systems (such as GC's) and composite systems (such as S0's and ellipticals). This will be discussed further in §3.

2.2. Composite Stellar Populations

Galaxies are known to be composed of more than a simple stellar population (i.e. single age and metallicity). This is clearly the case for the Milky Way, based on studies of nearby stars (Twarog 1980). And metallicity gradients in ellipticals demonstrate that they too are composed of stars with a range

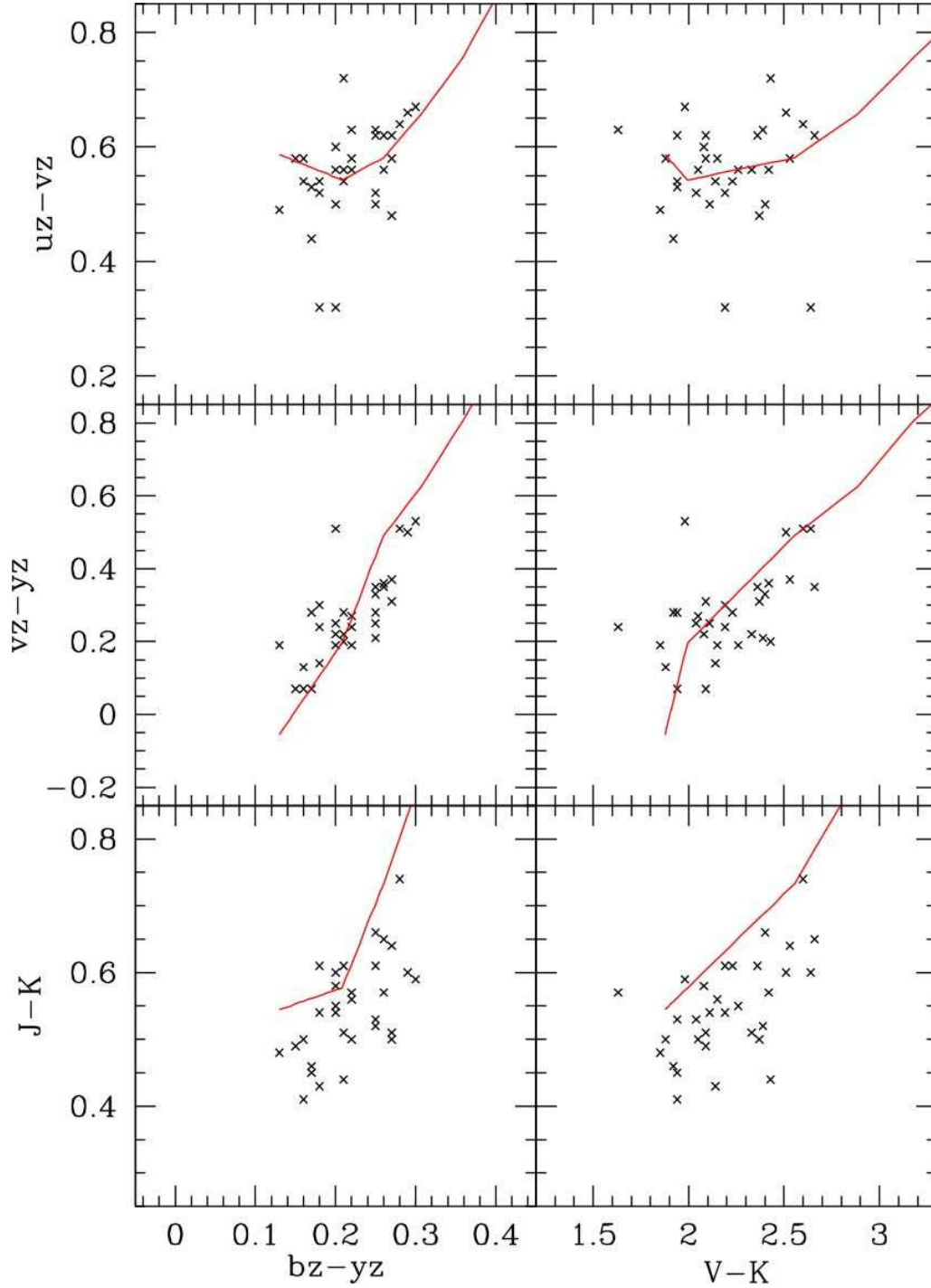


Fig. 1.— The optical and near-IR color-color diagrams for Galactic globular clusters (Rakos & Schombert 2005). As these clusters are nearly coeval in age, the correlations in color reflect metallicity variations between the clusters. Also shown are the 12 Gyr SSP models from Bruzual & Charlot (2003). The models are an excellent match to the data except for the $J - K$ colors (for unknown reasons). Scatter around the models is fully explained by stochastic variation in color due to the number of stars at the tip of the RGB and AGB.

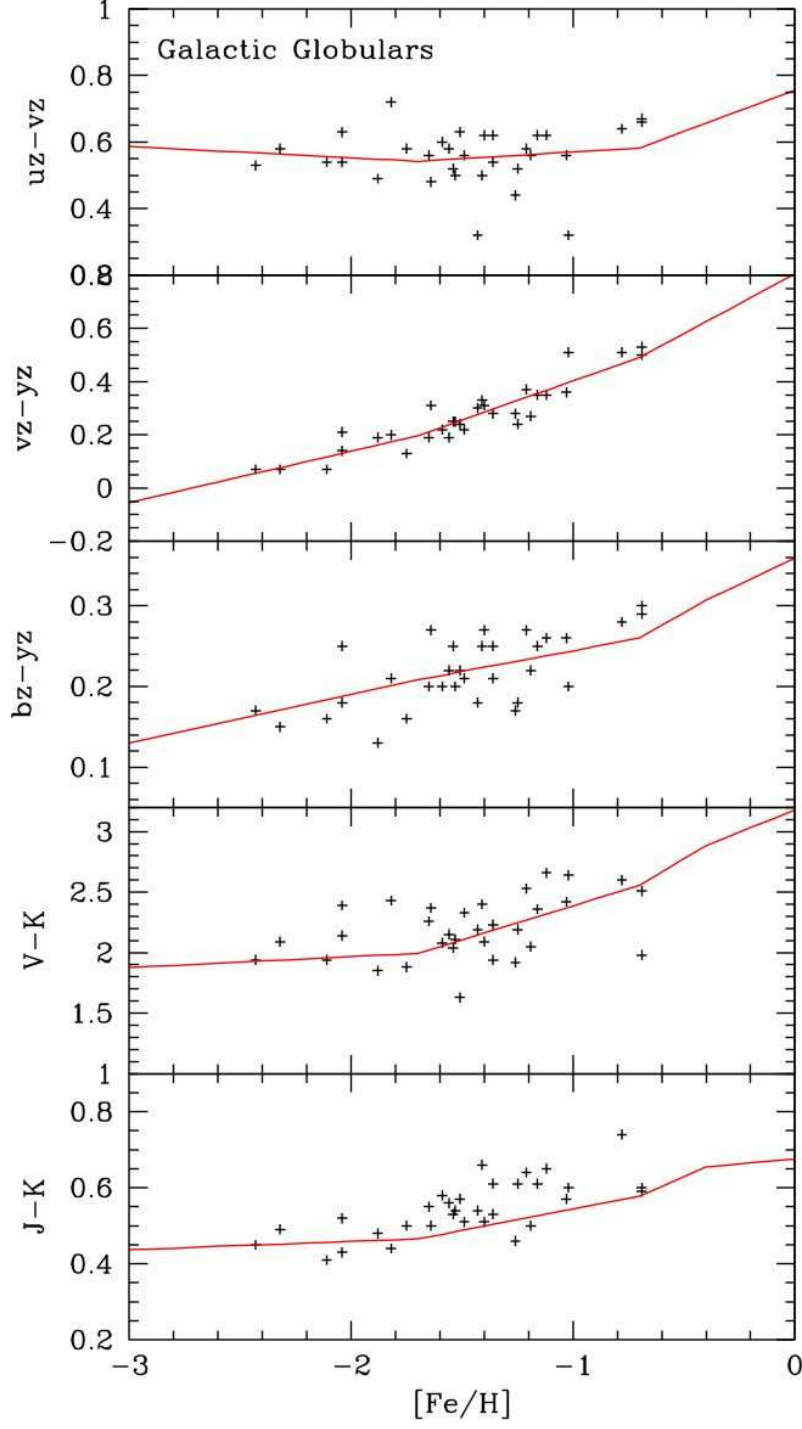


Fig. 2.— Optical and near-IR colors versus metallicity ($[\text{Fe}/\text{H}]$) for 32 Galactic globulars. The tightest correlation between color and $[\text{Fe}/\text{H}]$ is found for the narrowband color, $vz - yz$. The $uz - vz$ color is influenced by hot HB stars and the second parameter effect. The $bz - yz$ color lacks sufficient metal lines for a stronger correlation. Also shown are the 12 Gyr SSP models.

of metallicities (Sanchez-Blazquez *et al.* 2006). With respect to integrated optical and near-IR colors, ellipticals have colors that are clear extrapolations from SSP colors, such as galactic globulars, but have significant differences that demonstrate that they are composed of stars with a range of metallicities. For example, the mid-ultraviolet region of an elliptical’s spectra are best modeled by an old metal-rich plus smaller old metal-poor populations (Bressan, Chiosi & Fagotto 1994, Rose & Deng 1999, Lotz, Ferguson & Bohlin 2000).

This composite color effect is best seen in Figure 3, a plot of our optical $vz - yz$ and $bz - yz$ colors and the near-IR color $V - K$. The globular cluster data from Figure 2 is replotted along with a BC03 12 Gyr SSP models, a good match to the GC data. Also shown are the colors of 50 bright ellipticals in the core of the Coma cluster. The optical colors for the Coma sample derive from Odell, Schombert & Rakos (2002), the near-IR colors for the same galaxies are taken from Eisenhardt *et al.* (2007). While the SSP models are a good fit to the GC data, they do not fit the elliptical colors. The deviations from an SSP model are such that ellipticals have $vz - yz$ colors that are slightly bluer than single metallicity models (Rakos, Schombert & Odell 2008). This is exactly what one would expect by ignoring the contribution of low metallicity stars and a simple model that considers a range of metallicities is shown as a dashed line in Figure 3. A slightly younger SSP (7 Gyrs in Figure 3), would match the optical colors, but fail to match the near-IR colors. While this simple composite model will be discussed in greater detail below, it demonstrates that elliptical colors are best explained by a composite of underlying metallicities, an obvious conclusion based on population studies of our own Galaxy.

Decoding the color of galaxies requires a map of the ages of the stellar populations and their metallicity distribution (as a function of age). For the purposes of this initial examination of a galaxy’s underlying metallicity distribution, we will assume that all the color change in their integrated luminosity is due solely to metallicity effects. There are many reasons to believe that a majority of the stars in ellipticals are old ($\tau > 10$ Gyrs) ranging from the tight correlation of the color-magnitude relation to the red envelope in high redshift studies of clusters. In a parallel paper (Schombert & Rakos 2009), we present a detailed analysis of spectroscopic determination of galaxy ages as it impacts on the observed color properties of ellipticals, i.e. the color-magnitude relation (CMR). Spectroscopic studies find a high fraction of ellipticals with ages less than 7 Gyrs (see review by Schiavon 2007); however, these ages are in conflict with the colors of early-type galaxies. Detailed comparison to the CMR demonstrates that early-type galaxies with ages less than 7 Gyrs are rare and we have ignored galaxy age from our analysis.

2.3. Chemical Evolution Models

In order to model galaxy integrated colors, we will need to combine the predicted colors from the SED models with a model of the internal metallicity distribution, the so-called metallicity distribution function (MDF, Pagel 1997). The mean metallicity, Z , of a galaxy will then be a luminosity weighted sum of the contribution from a continuum of metallicities. And it is expected that the peak Z value will vary with position in the galaxy (i.e. gradients) and with the mass of the galaxy, such that higher mass galaxies process more material before the onset of galactic winds overcomes their gravitational potentials to halt star formation and further enrichment.

There are only a few galaxies with actual MDF’s measured from HST imaging of the tip of the

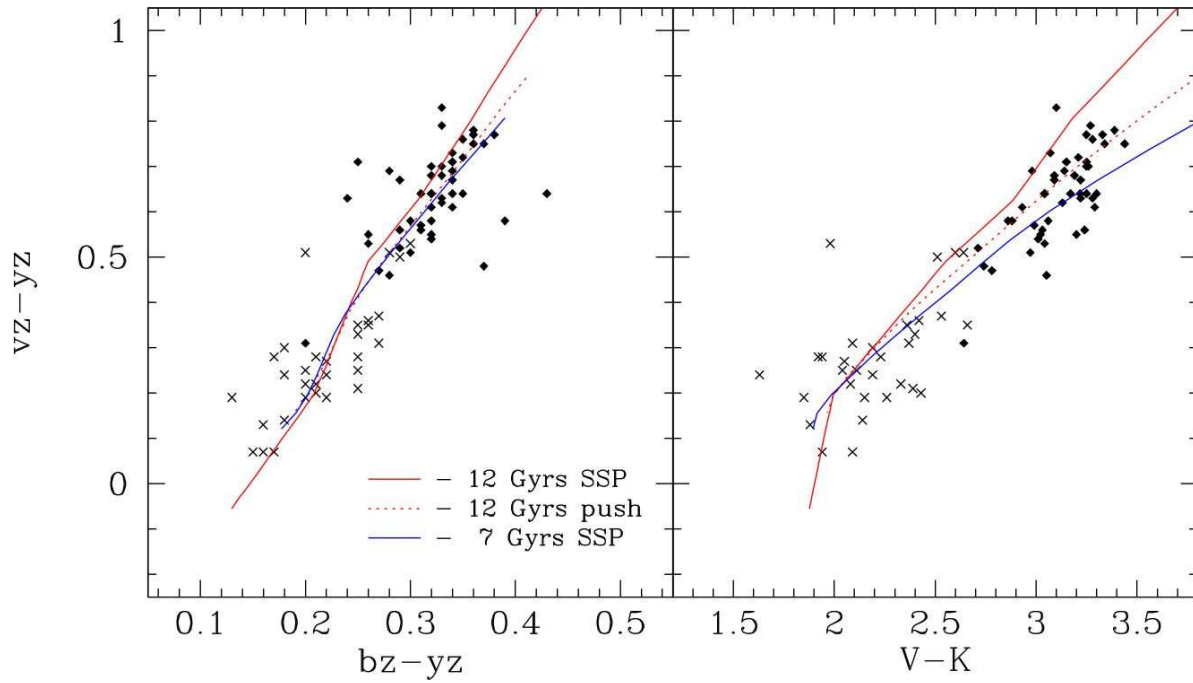


Fig. 3.— Optical and near-IR color-color diagrams for globular clusters (crosses) and Coma ellipticals (solid symbols). The solid red line is a 12 Gyr SSP model, the blue line is a 7 Gyr SSP model. While the GC data is adequately described by the SSP models, a majority of ellipticals lie to the right of the 12 Gyr model. The dashed line is a composite stellar population (CSP) model, for a 12 Gyr population using a simple infall chemical enrichment scenario. While a younger model can explain the optical colors, a composite population is a better match to both the optical and near-IR elliptical data. While the colors of ellipticals are extensions of globular cluster colors, these slight differences are best explained by a CSP model.

RGB. The most relevant examples to this study are the old populations in M31 (Worthey *et al.* 2005) and the nearby elliptical NGC 5128 (Harris & Harris 2000). Both studies display MDF’s with several features in common; 1) a well defined gaussian-like peak, 2) a long tail to low metallicities, 3) a sharp cutoff on the high metallicity side. Both galaxies display a lower metallicity peak with increasing radius from the galaxy center (i.e. metallicity gradients). This results in a narrower MDF at lower peak metallicities.

The simplest model of chemical evolution to produce a MDF is, of course, the closed-box enrichment scenario (van den Bergh 1962). This scenario assumes no infall or outflow of gas and the metallicity of the stars increases in yield with every epoch of star formation. The solution for this model is analytic and displayed in Figure 4.

A well know problem for closed-box model is that it over estimates the number of low metallicity stars ($Z/Z_{\odot} < 0.3$), the so-called G dwarf problem (Gibson & Matteucci 1997). This over estimation occurs not only for stars in the local solar neighborhood (van den Bergh 1962, Schmidt 1963) but also in the MDF’s in nearby galaxies (Sarajedini & Jablonka 2005, Worthey *et al.* 2005). The standard solution is to allow for an nonzero initial abundance for the gas that produces the first generation of stars or a prompt enrichment mechanism. A simple shift of initial abundance has been demonstrated to be a poor fit for M31 and other nearby galaxies (Harris & Harris 2000, Sarajedini & Jablonka 2005); however, an accreting box scenario (a relaxing of the infall constraint, Harris & Harris 2000, dashed line) has been more successful and also lends itself to an analytic solution. For comparison to these models, we have replotted the inner MDF of NGC 5128, a nearby elliptical (Harris & Harris 2000) in Figure 4. Neither of these two models are a particularly good match to the data.

A more recent model is given by an infall scenario (Kodama & Arimoto 1997). This model has the advantage of linking the accretion rate to the star formation rate, a more physically realistic scenario, and yielding a constant gas mass. This model is shown in Figure 4, but also suffers from an over abundance of metal-poor stars as compared to observations. Adjustments to lower the number of metal-poor stars only results in an over production of metal-rich stars, although the general shape of the infall MDF follows the trend of the data. This is primarily due to the instantaneous mixing assumption for these models which smooths the production of metals over space and time allowing for more metal-poor stars. In reality, one would expect regions of high metallicity to form, which would produce a fast enrichment sequence.

The G-dwarf problem led us to consider a modification to the infall or accreting models in a completely artificial fashion to match the MDF in NGC 5128. This modification, which we call the ‘push’ model, is a simple reduction of the low metallicity end of the infall model. To preform this reduction, we adopt an infall model’s shape, a peak metallicity with a sharp high metallicity cutoff and a long low metallicity tail. This metallicity distribution’s peak $[\text{Fe}/\text{H}]$ is adjusted to alter the total mean metallicity. Our push model artificially reduces the low metallicity end of this distribution, simply by a linear reduction while keeping the total normalization constant (i.e. we push down the number of low Z stars per mass bin). For our experiments herein, adequate fits to the data were obtained with less than a 30% reduction of the low metallicity side.

There is no direct theoretical or model support for our push model (although it forces a relaxation of the instantaneous mixing assumption), it is simply done to explore the effect of fewer low metallicity stars on the integrated colors. However, we note that the shape of the push model reproduces the MDFs

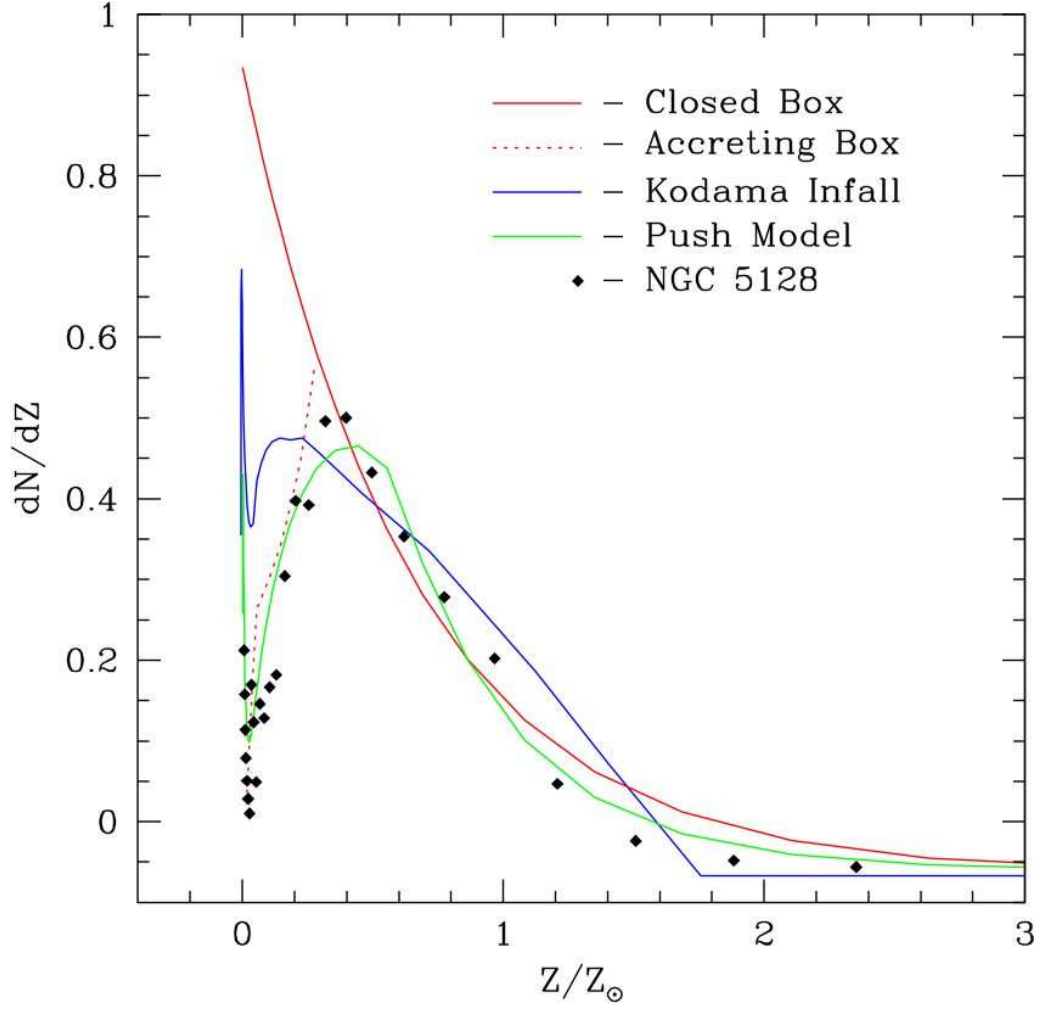


Fig. 4.— Comparison of various chemical enrichment models. The closed box model is shown as a solid red line (with an initial enrichment as a red dashed line). An infall model (Kodama & Arimoto 1997) is shown as a solid blue line (see Yi *et al.* 1998). Our analytic ‘push’ model, designed to artificially reduce the metal-poor component, is shown as a solid green line. All these models are compared to the metallicity data for the elliptical NGC 5128 (inner regions, Harris & Harris 2000).

produced by inhomogeneous enrichment models (Malinie *et al.* 1993, Oey 2000), where star formation occurs in discrete patches throughout a galaxy and only allowed to mix between star formation episodes. This increases the amount of mixing and results in fewer metal-poor stars. As we can see in Figure 4, this type of model (with a 30% reduction of metal-poor stars) produces the best ‘french curve’ through the NGC 5128 data. Although our push model lacks a physical foundation, we note that the inhomogeneous models also lack any simple parameterization that relates to known galaxy properties and has a large number of unconstrained variables.

3. [Fe/H] Determination from the $\langle \text{Fe} \rangle$ Index

As stated in the Introduction, the power to line indice measurements (e.g. the Lick/IDS system) is their direct determination of an element’s abundance. One of the clearest measures of global metallicity, as outlined in Trager *et al.* (2000), is the $\langle \text{Fe} \rangle$ index, the numerical average of the Fe5270 and Fe5335 lines. This feature measures Fe, C, Mg, Ti, Si and, thus, will be mildly sensitive to changes in the ratio of α elements to Fe. However, for the samples we have chosen (see below) the variation in α/Fe is small and will be ignored.

The $\langle \text{Fe} \rangle$ index has been used by numerous studies of metallicity and age in galaxies, but we have selected our sample, for comparison to our narrowband colors, from three studies of early-type galaxies; Trager *et al.* (2000), Poggianti *et al.* (2001) and Thomas *et al.* (2005). Our choice of these datasets is for a number of practical reasons. One, the Trager *et al.* work was a clear and strong step forward in the use of the Lick/IDS system for galaxy work and sets the standard for age and metallicity determination in that spectral system. The Poggianti *et al.* study was on Coma cluster galaxies where we have matching narrowband and near-IR colors (Rakos & Schombert 2008). The Thomas *et al.* study is one of the most recent, and largest, work with published $\langle \text{Fe} \rangle$ values. The total sample contains 185 galaxies of which we have matching color data for 119 galaxies. For the remaining 72 galaxies, we have estimated their $vz - yz$ colors using their absolute M_{5500} luminosity and the color-magnitude relation (Odell, Rakos & Schombert 2002), although their exclusion from the analysis does not change our results.

The resulting plot of $\log \langle \text{Fe} \rangle$ versus metallicity color ($vz - yz$) is shown in Figure 5. Also plotted are the BC03 SSP models for ages of 4 and 12 Gyrs. What is immediately obvious from this plot is that a majority of the metallicity data lies above and/or to the left of the SSP models. As the SSP models accurately match the globular cluster color and metallicities, then we might at first interpret the difference in Figure 5 as due to the composite nature of elliptical stellar populations. However, this diagram implies, logically, only that ellipticals are either 1) bluer in $vz - yz$ color per metallicity value or 2) more metal-rich per integrated color bin. And these regions of the color-metallicity diagram could be occupied for various star formation reasons.

For the first option, a bluer $vz - yz$ color can be derived at a constant metallicity by a younger mean population, i.e. less than 4 Gyrs in age. We discuss the impact of younger stars in a later paper (Schombert & Rakos 2009); however, to summarize that work, in order to match the color values in Figure 5, the mean age of the entire underlying stellar population in a majority of ellipticals would be required to be less than 2 Gyrs. This is extremely young for a total stellar population (although there may be small numbers of young stars in ellipticals, see Trager *et al.* 2000) and is not apparent in any

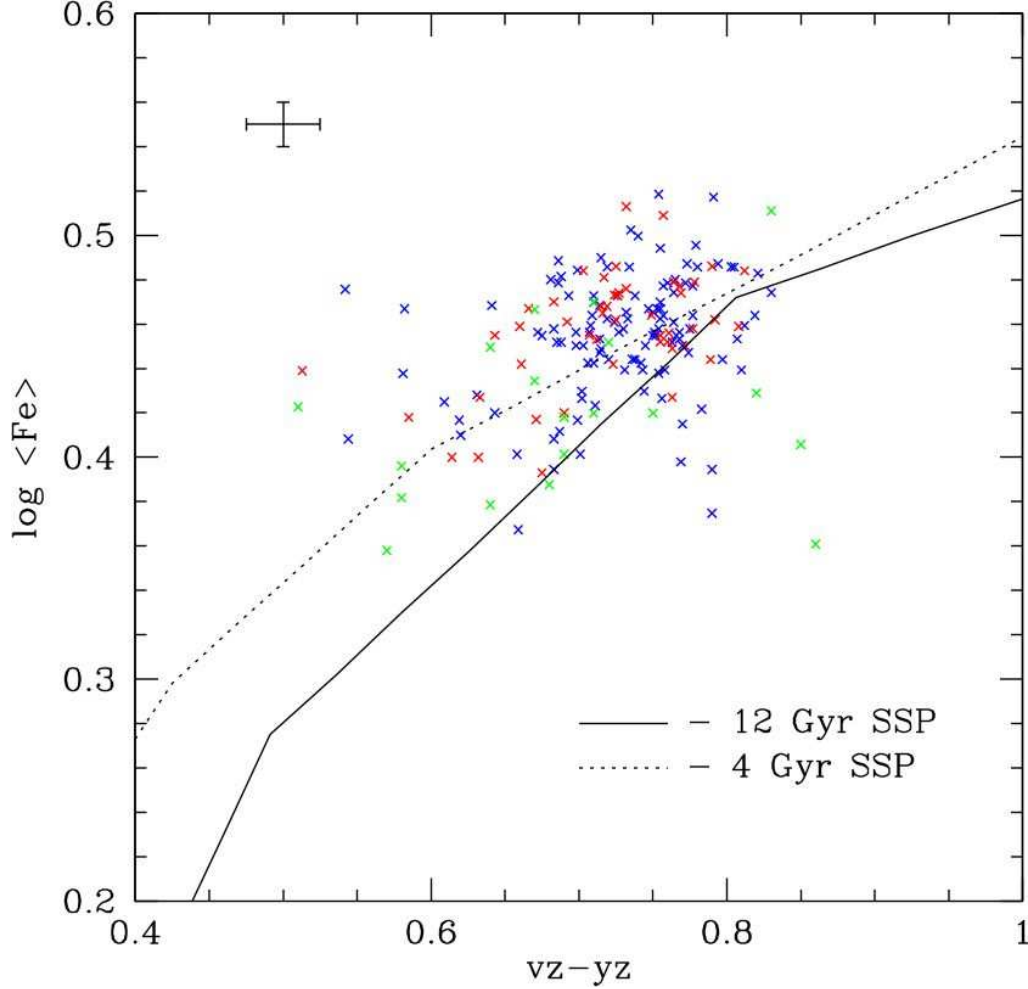


Fig. 5.— The $\langle \text{Fe} \rangle$ index from the Lick/IDS system versus galaxy narrowband color, $vz - yz$. The $\langle \text{Fe} \rangle$ index is considered the most accurate direct measure of the metallicity of a stellar population. In contrast, $vz - yz$ measures the mean metallicity color of a galaxy, a value that is dominated by the effect of metallicity on the position of the RGB. Blue symbols are data from Thomas *et al.* (2005), red symbols are from Trager *et al.* (2000) and green symbols are Coma galaxies (Mobasher *et al.* 2001). The solid line is a 12 Gyr SSP model from Bruzual & Charlot (2003), the dashed line is a 4 Gyr model. The SSP models clearly do not fit the metallicity data leading us to conclude that galaxies are either more metal-rich for their color or too blue for their metallicity. As integrated color is more sensitive to the contribution of metal-poor stars than the $\langle \text{Fe} \rangle$ index, then a majority of the deviation from the SSP line is due to color. This diagram demonstrates that an SSP model is an incomplete description of the colors of galaxies and a chemical evolution scenario is required.

other color system or spectral indicator. In addition, it would imply that a majority of ellipticals in intermediate redshift clusters ($0.3 < z < 0.7$) have star-forming colors, which is clearly not seen (Rakos & Schombert 1995).

The other logical option is that the metallicity indicator $\langle \text{Fe} \rangle$ is simply measuring a different quantity in galaxies than the integrated color $vz - yz$, in this case a higher metallicity than indicated by the integrated color. This might be true due to the geometry of the data sampling, as spectral values are based on core luminosities whereas the metallicity color, $vz - yz$, is based on the total galaxy light. Strong metallicity gradients would result in a noticeable difference for metallicity values determined by core light versus halo light. In addition, composite populations of varying metallicity may sum up in differing ways for $\langle \text{Fe} \rangle$ versus color (i.e. in particular the contribution from hot BHB stars or a metal-poor MS turnoff population, see Worthey, Dorman & Jones 1996). We will explore both these effects in the next two sections.

4. Aperture Correction to $\langle \text{Fe} \rangle$

A key difference between line indice studies and color work is observational in that line indices, using the Lick/IDS system, are determined by the smaller angular sized slit or fiber spectroscopy. The typical slit sizes are such that a line indice measurement of a particular galaxy is going to be confined to the central regions. Thus, due to the geometry of the observational technique and the fact that spectroscopic data is surface brightness weighted, the galaxy light obtained by line indices studies will be heavily weighted towards the core regions. Since early-type galaxies have clear color gradients (Sanchez-Blazquez *et al.* 2006), which are known to be primarily due to metallicity gradients, this leads to the possibility that line indice values are biased towards higher metallicity values. Thus, the comparison of line indice values to global colors, those determined by the average metallicity as given by the entire luminosity of the galaxy, may be invalid.

While it seems obvious that some bias towards higher metallicity values exists in line indice studies, the amount of bias is unknown and may be negligible. Certainly, as colors gradients are known to be small in early-type galaxies (Sandage & Visvanathan 1978, Peletier *et al.* 1990, Schombert *et al.* 1993), there is an expectation that with sufficient areal coverage (e.g. over $1/3$ an effective radius) the difference between a global metallicity value and one determined from spectroscopy will be small.

In order to estimate the metallicity bias for spectroscopic work due to an aperture correction, we consider the Coma observations of Poggianti *et al.* (2001) described in Mobasher *et al.* (2001). This data was taken with a fiber spectrograph with 2.7 arcsec slits (for comparison, SDSS uses three arcsec fiber diameters). At the redshift of Coma, this corresponds to a diameter of 1.2 kpc. For an L_* galaxy, the light measured through this aperture corresponds to approximately $1/3$ the total light of the galaxy. This will be less for brighter galaxies (larger effective radii) and more for lower luminosity galaxies resulting in a variation of about 20% for the luminosity range given by the Poggianti *et al.* sample.

With the existence of color gradients, this smaller fraction of total light measured by fiber slits will also contain a redder (more metal-rich) stellar population. Using the color gradients for our narrowband color, $vz - yz$ (Schombert *et al.* 1993), we find that gradients take on a range of values. Galaxies with strong gradients (e.g. NGC 4374) have values of $\Delta(vz - yz)/\Delta(\log r) = -0.15$. Galaxies with weak

gradients (e.g. NGC 7562) have values near -0.05 . This results in differences for mean color between the core luminosity seen by slits and total color as $+0.09$ for strong gradients to $+0.03$ for weak gradients. Converting this color difference into $[\text{Fe}/\text{H}]$ (using BC03 12 Gyr SSP’s) leads to $[\text{Fe}/\text{H}]$ values being 0.25 to 0.09 dex higher for spectroscopic measurements compared to values deduced from a galaxy’s total light. Thus, on average, the Lick/IDS values need to be lowered by approximately 0.15 dex to represent the mean $[\text{Fe}/\text{H}]$ of a galaxy as a whole, which corresponds to a change of 0.04 in the $\log \langle \text{Fe} \rangle$ index.

5. Multi-Metallicity Population Correction to $[\text{Fe}/\text{H}]$

A second correction to consider is that the value measured by colors is, of course, a luminosity weighted integrated value. Comparison to models has always assumed that the underlying stellar population is simple (i.e. SSP). There is every expectation that this is false based on any chemical enrichment models which predicts a spread in metallicity. In addition, HST imaging has demonstrated broad MDF’s in nearby galaxies (Worthey *et al.* 2005).

Again, using the SED models from Bruzual & Charlot (2003) combined with an infall scenario of chemical enrichment (Kodama as described in Yi *et al.* 1998), we can estimate the difference between the numerical averaged $[\text{Fe}/\text{H}]$ (actual sum of the metallicities of the stars) versus the luminosity weighted value, $\langle \text{Fe}/\text{H} \rangle$. A series of simulations were run using this formula where the only variable in this simulation is the peak $[\text{Fe}/\text{H}]$ which is allowed to vary from -2.5 to $+0.5$. The shape of the MDF is fixed, starting at $[\text{Fe}/\text{H}] = -2.5$ and linearly adjusted to the peak $[\text{Fe}/\text{H}]$. This MDF is then convolved with the SED models to produce colors for a composite stellar population (CSP). The output values from the CSP model are the luminosity weighted $\langle \text{Fe}/\text{H} \rangle$, what one would measure from the integrated light and the actual numerical average metallicity, $[\text{Fe}/\text{H}]$, from the sum of the stars by mass. For an SSP, or stellar population with a very narrow range of metallicities, these values would be equivalent. But for a stellar population with a wide range of metallicities (in particular, a long low metallicity tail), each metallicity bin contributes a slightly different luminosity per mass (higher for lower $[\text{Fe}/\text{H}]$ values) and, thus, the resulting observed $\langle \text{Fe}/\text{H} \rangle$ value does not match the actual underlying metallicity of the population by mass. Since a metal poor population is more luminous than the metal-rich population by mass, then a luminosity weighted value of $[\text{Fe}/\text{H}]$ will underestimate the true value (Arimoto & Yoshii 1987).

A series of conclusions were reached from comparing the values of a luminosity weighted metallicity and the actual metallicity by stellar number. First, the exact shape of the MDF has little effect on the correlation between average $[\text{Fe}/\text{H}]$ and the luminosity weighted $\langle \text{Fe}/\text{H} \rangle$ as long as there is a low metallicity component to the model. Second, a metal-poor tail is a requirement to the model as any distribution without a metal-poor component failed to match the galaxy colors (e.g. the color-magnitude relation). Third, the relationship between the actual mean $[\text{Fe}/\text{H}]$ and the luminosity weighted (i.e. observed) metallicity is linear and easy to calculate. A correction can be defined between an observed $[\text{Fe}/\text{H}]$ value ($\langle \text{Fe}/\text{H} \rangle$) and the true value which is expressed as:

$$[\text{Fe}/\text{H}] = 1.063 \langle \text{Fe}/\text{H} \rangle + 0.099$$

Not to surprisingly, the inclusion of a metal poor tail to a metallicity distribution causes the

observed colors converted into a $[\text{Fe}/\text{H}]$ value (usually calculated from SSP models) to underestimate the real numerical averaged $[\text{Fe}/\text{H}]$. Thus, for solar metallicities, the observed $[\text{Fe}/\text{H}]$ must be adjusted upward by approximately 0.1 dex. Interestingly, this upward correction to $[\text{Fe}/\text{H}]$ is almost exactly balanced by a downward correction needed for aperture corrections to line indice work (see previous section) which would explain the high consistence between various studies.

Lastly, we can ask of the simulations the typical difference a metal-poor component makes on the observed values of the $\langle\text{Fe}\rangle$ index versus colors. In the examples above, the typical change in color was on the order of 25% for a CSP model versus a SSP. On the other hand, the corresponding change in $\langle\text{Fe}\rangle$ was only 10%. What this implies is that observed colors are more strongly influenced by the hot component of a metal-poor population (BHB stars), whereas the $\langle\text{Fe}\rangle$ index derives most of its luminosity from the RGB stars.

To summarize, the metallicity line indice, $\langle\text{Fe}\rangle$, will suffer from both an aperture effect, due to galaxy metallicity gradients, and an over estimate of mean metallicity due to the use of SSP models with only a single metallicity. However, these two effects balance one another such that the $\langle\text{Fe}\rangle$ index is a good measure of the mean $[\text{Fe}/\text{H}]$ of a galaxy’s stellar population. Colors, on the other hand, being a total measure of the integrated light of a galaxy, require a correction to estimate the mean $[\text{Fe}/\text{H}]$ since they will display the overall color of the composite stellar population. The correction is simple, dependent only weakly on the assumed chemical enrichment model. These effects also allow for an opportunity to measure the effect of a composite population by comparing $\langle\text{Fe}\rangle$ values with a galaxies integrated color.

6. Chemical Enrichment Interpretation of Color versus $[\text{Fe}/\text{H}]$

Metallicity determination by colors requires an intermediary step, either calibration by comparison to SED models or comparison to a standard system such as galactic globulars. For our continuum color system, the $vz - yz$ color is the metallicity indicator of choice since it has a linear relationship with $[\text{Fe}/\text{H}]$ that varies only slightly with age, as long as the stellar population is older than 5 Gyrs (Rakos & Schombert 2008). For some subset of all three $\langle\text{Fe}\rangle$ samples we have matching narrowband photometry of the same galaxies for direct comparison. These objects are shown as data points in the following Figures, where the Thomas *et al.* sample is shown as blue points, Trager *et al.* as red and Poggianti *et al.* as green.

In order to test a CSP model of chemical enrichment, we have collected, as discussed in §3, a direct measure of $[\text{M}/\text{H}]$ of the underlying stellar population through the $\langle\text{Fe}\rangle$ index and color for the underlying stellar population as produced, primarily, by the mean $[\text{M}/\text{H}]$ in our $vz - yz$ narrowband photometry. As discussed in §4 and 5, there are corrections to be made to spectroscopic values to account for aperture effects and a metal-poor component. However, since the aperture corrections were matched by opposing luminosity corrections (see §5), no change was made to $\langle\text{Fe}\rangle$ data, and $\langle\text{Fe}\rangle$ was converted to $[\text{M}/\text{H}]$ using the prescriptions outlined in Trager *et al.* (2000). We will adopt these values as the mean metallicity of the entire galaxy, a numerical average. The model tracks for the various chemical enrichment scenarios will use a mean metallicity versus a luminosity weighted color, as the integrated colors reflect the entire underlying stellar population.

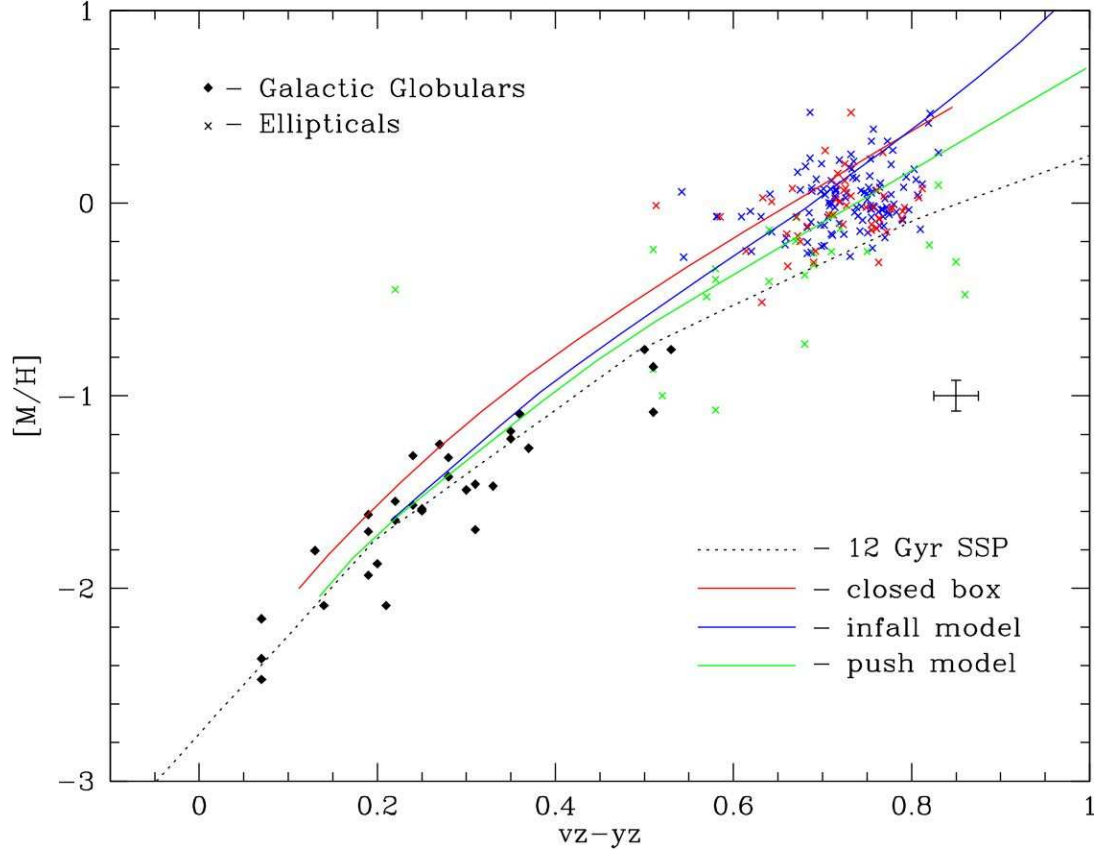


Fig. 6.— The mean metallicity of a galaxy, $[M/H]$, versus metallicity color, $vz - yz$. Galactic globulars are solid symbols, galaxies are crosses using the same color scheme as Figure 5. A black dashed line represents a 12 Gyr SSP model, which is an excellent fit to the galactic globulars, but fails for ellipticals. The closed box and infall models are shown as solid red and blue lines. The closed box model fails to match the data, the infamous G-dwarf problem, however, even the infall model appears to overproduce metal-poor stars. The best fit is found with our ‘push’ model, and artificial suppression of the metal-poor tail to match the shape of the MDF produced by inhomogeneous models (Oey 2000).

The resulting plot of metallicity ($[M/H]$) versus galaxy color ($vz - yz$) is shown in Figure 6. The color-metallicity relation (i.e. mass-metallicity relation) is evident even though the mass range of the sample is limited. Also plotted are the data for Galactic globular clusters (Rakos & Schombert 2005). The SSP models for a 12 Gyr population of various metallicities are shown as a dashed line. While these models are excellent fits to the GC data, they fail to describe the galaxy data. A vast majority of the galaxy data lie to the blueward side of the SSP models indicating, again, that galaxies must be composed of a significant, at least in luminosity, population of metal-poor stars.

The first chemical enrichment model to test is the closed box model as outlined in Sarajedini & Jablonka (2005) and shown as the red track in Figure 6. Of course, the immediate result of an enrichment model is the addition of low metallicity stars to the integrated stellar population. Using our CSP technique of summing a mixed stellar population, we find, not surprisingly, that the integrated $vz - yz$ colors are bluer for a closed box scenario than for a single metallicity SSP. However, the closed box track in Figure 6 is clearly too blue compared to the data on ellipticals. This is the famous G-dwarf problem (Pagel & Patchett 1975), the known deficiency of low metallicity stars in the solar neighborhood. This deficiency has also been noted in Milky Way halo populations (Tantalo *et al.* 1996), populations in M31 (Worthey *et al.* 2005) and NGC 5128 (Harris & Harris 2000). The usual resolution is to modify the closed box assumption with a model that has an initial enrichment component and an inflow of metal-poor gas, an infall model.

The infall model assumes that gas flows into a system while the epoch of star formation is still ongoing. Thus, the gas is replenished at the same rate as star formation consumes it (Gibson & Matteucci 1997). For our purposes, we adopted the Kodama infall model outlined in Yi *et al.* (1998). We parameterized the models over galaxy mass by sliding the metallicity distribution shape over the metallicity range $[M/H] = -2$ to $+1$ as described in Rakos *et al.* (2001). The resulting CSP models using an infall scenario of varying total mass is shown as the blue line in Figure 6. While the infall model reduces the number of metal-poor stars, and thereby reddening the predicted $vz - yz$ colors, this effect does not match the elliptical data.

The failure of the infall model, in that it still appears to produce too many metal-poor stars per gas mass, motivated us to produce a model which suppresses the low metallicity tail. We refer to this model as the ‘push’ model as it pushes down the low end of the metallicity curve (see §2.3). However, this is a completely artificial change to the infall model, and has no physical basis other than it results in the color changes needed to match the data. Our push model, shown in Figure 6 and the resulting color-metallicity track is shown in green in Figure 6, is a good match for the data with a 30% reduction to the metal-poor component. This agrees well with our push model fit to the NGC 5128 data, a similar morphology type to our elliptical sample. This also confirms that the G-dwarf problem is even more severe in ellipticals than spirals such as the Milky Way and M31 (Worthey, Dorman & Jones 1996).

A sharp reduction of the low metallicity end of a galaxy’s MDF is a feature to inhomogeneous enrichment models. These models relax the chemical homogeneity assumption by adopting a fixed dispersion in metal production. Following the paradigm of Oey (2000), these models are parameterized by two variables 1) the number of generations of star formation and 2) the filling factor in the ISM that each generation occupies. As noted in the Oey study, an old, metal-rich population is achieved by a high filling factor. To reproduce our push model values would require a low number of star formation generations, i.e. a rapid and short initial star formation epoch for ellipticals in agreement with the

conclusions based on α/Fe ratios and galaxy mean ages (Rakos, Schombert & Odell 2008).

7. Conclusions

Combining information from spectroscopic measurements of galaxy cores with narrowband colors allows for a test of two, relatively independent, estimators of mean metallicity. For example, spectroscopic lines measure key metallicity lines (e.g. Fe) directly, whereas, colors measure the effect of changing metallicity on temperature of the stellar population’s atmospheres (primarily the position of the RGB in an HR diagram). This different sensitivity to metallicity can be exploited to test predicts from chemical enrichment models on the shape of the MDF.

We summarize our results as follows:

- We have examined the accuracy of SED models on predicting narrowband and near-IR colors in globular clusters, simple stellar populations of singular age and metallicity. We find that our optical colors and $V - K$ are well matched by SED models; however, near-IR colors (i.e. $J - K$) do not follow SSP tracks.
- The most accurate measure of metallicity (e.g. $[\text{Fe}/\text{H}]$) is our narrowband $vz - yz$ color. Based on arguments in Schombert & Rakos (2009), the range of galaxy ages from 8 to 13 Gyrs has a negligible effect on the $[\text{Fe}/\text{H}]$ versus $vz - yz$ correlation. In addition, Schombert & Rakos (2009) rejects the proposal that a majority of galaxy ages in clusters are of less than 8 Gyrs. Thus, for this limited set of galaxy morphology (early-type), we can use the $vz - yz$ color as a sole measure of integrated $[\text{Fe}/\text{H}]$ in a composite stellar population.
- Comparison of optical and near-IR elliptical colors demonstrates that early-type galaxies are best explained by a composite stellar population. As we reject extremely young mean galaxy ages, then, in order to match the colors of ellipticals, the underlying stellar population must be singular in age but with a range of internal metallicities.
- There is a well defined continuum between $vz - yz$ color and metallicity ($[\text{M}/\text{H}]$) where the colors of ellipticals are bluer than that predicted by SSP models. The inclusion of a metal-poor stellar population is an obvious solution, where the fraction of metal-poor stars can be estimated from a chemical evolution scenario.
- The simplest chemical evolutionary scenarios, the closed box model and the initial enrichment model can be rejected as solutions to the MDF in ellipticals due to their over production of metal-poor stars (and resulting blue integrated colors). This results in the infamous G-dwarf problem (Pagel & Patchett 1975), a well known problem for the local stellar neighborhood and stellar populations in nearby galaxies. Our data indicates that the G-dwarf problem is universal (Worthey, Dorman & Jones 1996).
- Infall models, while a better match to the data, also over produce metal-poor stars and lie on the blue side of the data. Our analytic ‘push’ model is a artificially constructed curve that suppresses the number of metal-poor stars to the typical infall model. This MDF shape, narrower at its peak, reduced on the metal-poor end and sharper on the metal-rich end, matches the elliptical galaxy

data. These types of curves are also predicted by inhomogeneous models of chemical evolution (Tinsley 1975, Malinie *et al.* 1993, Oey 2000) with high filling factors and rapid initial epochs of star formation.

A key missing piece of the chemical evolution puzzle in ellipticals is the age-metallicity relationship (AMR). The AMR would provide a detailed breakdown of the evolution of the MDF, however, this information will be difficult to extract from composite systems such as distant ellipticals. Another avenue for exploration is the presence of metallicity gradients. With guidance by a galaxy formation scenario (matching our chemical enrichment scenarios), one could, ideally, match the metallicity distribution as a function of radius mapped into time. Future work with our narrowband system will concentrate on spatial analysis of nearby ellipticals to this very end.

Financial support from Austrian Fonds zur Foerderung der Wissenschaftlichen Forschung and NSF grant AST-0307508 is gratefully acknowledged. We thank all the various observatories which have supported our efforts, KPNO, CTIO and ESO. This research has made use of the NASA/IPAC Extragalactic Database (NED) which is operated by the Jet Propulsion Laboratory, California Institute of Technology, under contract with the National Aeronautics and Space Administration and has made use of data obtained from or software provided by the US National Virtual Observatory, which is sponsored by the National Science Foundation..

REFERENCES

- Arimoto, N., & Yoshii, Y. 1987, A&A, 173, 23
- Baade, W. 1944, ApJ, 100, 137
- Bressan, A., Chiosi, C., & Fagotto, F. 1994, ApJS, 94, 63
- Bruzual A., G. 2002, Extragalactic Star Clusters, 207, 616
- Bruzual, G., & Charlot, S. 2003, MNRAS, 344, 1000
- Cohen, J. G., Christlieb, N., McWilliam, A., Shectman, S., Thompson, I., Melendez, J., Wisotzki, L., & Reimers, D. 2008, ApJ, 672, 320
- Dolphin, A. E. 2002, Observed HR Diagrams and Stellar Evolution, 274, 450
- Eisenhardt, P. R., De Propriis, R., Gonzalez, A. H., Stanford, S. A., Wang, M., & Dickinson, M. 2007, ApJS, 169, 225
- Faber, S. M. 1972, A&A, 20, 361
- Gibson, B. K., & Matteucci, F. 1997, MNRAS, 291, L8
- Gilmore, G., Wyse, R. F. G., & Kuijken, K. 1989, ARA&A, 27, 555
- Girardi, L., Bressan, A., Bertelli, G., & Chiosi, C. 2000, A&AS, 141, 371

- Grebel, E. K. 2004, *Origin and Evolution of the Elements*, 234
- Harris, G. L. H., & Harris, W. E. 2000, *AJ*, 120, 2423
- Harris, J., & Zaritsky, D. 2004, *AJ*, 127, 1531
- Kodama, T., & Arimoto, N. 1997, *A&A*, 320, 41
- Lotz, J. M., Ferguson, H. C., & Bohlin, R. C. 2000, *ApJ*, 532, 830
- Malinie, G., Hartmann, D. H., Clayton, D. D., & Mathews, G. J. 1993, *ApJ*, 413, 633
- Matteucci, F. 2007, *From Stars to Galaxies: Building the Pieces to Build Up the Universe*, 374, 89
- Mobasher, B., et al. 2001, *ApJS*, 137, 279
- O’Connell, R. W. 1976, *ApJ*, 206, 370
- Odell, A. P., Schombert, J., & Rakos, K. 2002, *AJ*, 124, 3061
- Oey, M. S. 2000, *ApJ*, 542, L25
- Pagel, B. E. J. 1997, *Nucleosynthesis and Chemical Evolution of Galaxies*, by Bernard E. J. Pagel, pp. 392. ISBN 0521550610. Cambridge, UK: Cambridge University Press, October 1997.,
- Pagel, M. 1975, *Meteoritics*, 10, 469
- Peletier, R. F., Valentijn, E. A., & Jameson, R. F. 1990, *A&A*, 233, 62
- Pickles, A. J. 1985, *ApJ*, 296, 340
- Poggianti, B. M., et al. 2001, *ApJ*, 562, 689
- Rakos, K., Schombert, J., & Odell, A. 2008, *ApJ*, 677, 1019
- Rakos, K. D., & Schombert, J. M. 1995, *ApJ*, 439, 47
- Rakos, K., & Schombert, J. 2005, *PASP*, 117, 245
- Rakos, K., Schombert, J., & Odell, A. 2008, *ApJ*, 677, 1019
- Rakos, K., Maitzen, H., Prugovecki, S., Schombert, J. M., & Odell, A. 2001, *Galaxy Disks and Disk Galaxies*, 230, 363
- Rose, J. A., & Deng, S. 1999, *AJ*, 117, 2213
- Salaris, M., & Weiss, A. 1998, *A&A*, 335, 943
- Sánchez-Blázquez, P., Gorgas, J., Cardiel, N., & González, J. J. 2006, *A&A*, 457, 809
- Sandage, A., & Visvanathan, N. 1978, *ApJ*, 223, 707
- Sarajedini, A., & Jablonka, P. 2005, *AJ*, 130, 1627
- Schiavon, R. P. 2007, *ApJS*, 171, 146

- Schmidt, M. 1963, *ApJ*, 137, 758
- Schombert, J. & Rakos, K. 2009, in prep.
- Schombert, J. M., Hanlan, P. C., Barsony, M., & Rakos, K. D. 1993, *AJ*, 106, 923
- Schulz, J., Fritze-v. Alvensleben, U., Möller, C. S., & Fricke, K. J. 2002, *A&A*, 392, 1
- Skillman, E. D., Tolstoy, E., Cole, A. A., Dolphin, A. E., Saha, A., Gallagher, J. S., Dohm-Palmer, R. C., & Mateo, M. 2003, *ApJ*, 596, 253
- Smolčić, V., et al. 2006, *MNRAS*, 371, 121
- Tantalo, R., Chiosi, C., Bressan, A., & Fagotto, F. 1996, *A&A*, 311, 361
- Thomas, D., Maraston, C., Bender, R., & Mendes de Oliveira, C. 2005, *ApJ*, 621, 673
- Tinsley, B. M. 1975, *ApJ*, 197, 159
- Trager, S. C., Faber, S. M., Worthey, G., & González, J. J. 2000, *AJ*, 120, 165
- Twarog, B. A. 1980, *ApJ*, 242, 242
- Worthey, G., Dorman, B., & Jones, L. A. 1996, *AJ*, 112, 948
- Worthey, G., España, A., MacArthur, L. A., & Courteau, S. 2005, *ApJ*, 631, 820
- Yi, S., Demarque, P., & Oemler, A. J. 1998, *ApJ*, 492, 480
- van den Bergh, S., & Henry, R. C. 1962, *Publications of the David Dunlap Observatory*, 2, 281